Use of dipolar ^{1}H–^{15}N and ^{1}H–^{13}C couplings in the structure determination of magnetically oriented macromolecules in solution

Nico Tjandra[1,2], James G. Omichinski[1], Angela M. Gronenborn[1], G. Marius Clore[1] and Ad Bax[1]

Anisotropy of the molecular magnetic susceptibility gives rise to a small degree of alignment. The resulting residual dipolar couplings, which can now be measured with the advent of higher magnetic fields in NMR, contain information on the orientation of the internuclear vectors relative to the molecular magnetic susceptibility tensor, thereby providing information on long range order that is not accessible by any of the solution NMR parameters currently used in structure determination. Thus, the dipolar couplings constitute unique and powerful restraints in determining the structures of magnetically oriented macromolecules in solution. The method is demonstrated on a complex of the DNA-binding domain of the transcription factor GATA-1 with a 16 base pair oligodeoxyribonucleotide.

The principal source of geometric information used in NMR structure determination of macromolecules in solution lies in short (<5 Å) approximate interproton distance restraints derived from nuclear Overhauser enhancement (NOE) measurements[1,2]. NOE derived distances can also be supplemented by coupling constants (which are related to torsion angles), ^{13}C secondary shifts (related to the backbone ϕ and ψ angles) and ^{1}H shifts (which are influenced by ring current effects from aromatic groups, magnetic anisotropy of C=O and C–N bonds, and electric field effects arising from charged groups). All these parameters, however, are strictly local in nature and only define structural restraints between atoms immediately adjacent in the structure. Despite this limitation, protein structure determination by NMR is readily possible, primarily because short interproton distances between residues far apart in the sequence are conformationally highly restrictive.

Nevertheless, a key weakness in NMR structure determination to date has been the absence of restraints that can define long range order in their own right. Consequently, the relative positions of structural elements that do not have many contacts between residues far apart in the sequence are poorly defined using current NMR methodologies. Recently, it has been shown that the dependence of heteronuclear relaxation on rotational diffusion anisotropy can directly provide structural restraints that characterize long range order[3]. In practice, however, the method is only applicable to molecules with a significant diffusion anisotropy (> 1.5). In this paper, we demonstrate the utility of small residual one-bond ^{15}N–^{1}H and ^{13}C–^{1}H dipolar couplings to define the orientation of the N–H and C–H bond vectors relative to the molecule's magnetic susceptibility tensor, and hence provide an alternative set of restraints that characterize long range order. In addition, we show that they also improve local backbone stereochemistry.

Molecules with a non-zero magnetic susceptibility anisotropy will adopt a small degree of magnetic alignment in solution when placed in a magnetic field. As a result, dipolar couplings have a small, non-zero value, which scales with the square of the magnetic field strength[4,5]. These dipolar couplings contain information on the orientation of the internuclear vector relative to the molecular magnetic susceptibility tensor. For directly bonded ^{15}N–^{1}H and ^{13}C–^{1}H pairs, the dipolar couplings manifest themselves as small changes of the one-bond J splitting with increasing magnetic field strength. Recently, methods have been described which can measure such dipolar contributions in magnetically aligned proteins with a precision of a fraction of a hertz[6–8].

Dipolar couplings in proteins in isotropic solution were first reported for paramagnetic cyanometmyoglobin, and showed qualitative agreement with the crystal structure[9]. Subsequently, it was found that myoglobin dipolar couplings are about 30% smaller than expected on the basis of the magnetic susceptibility tensor calculated from the static crystal structure[10]. Although very large amplitude motions of intact helices in myoglobin were invoked as a possible explanation for this discrepancy[7], other causes such as small amounts of aggregation cannot be excluded[11]. Dipolar couplings measured in diamagnetic ubiquitin, which shows considerably weaker magnetic alignment, are in very good agreement with its crystal structure[7,8]. For both ubiquitin and myoglobin the dipolar couplings are consistent with the static crystal structures when the susceptibility tensor

[1]Laboratory of Chemical Physics, Building 5, National Institute of Diabetes and Digestive and Kidney Diseases, National Institutes of Health, Bethesda, Maryland 20892-0520, USA. [2]Laboratory of Biophysical Chemistry, Building 3, National Heart, Lung, and Blood Institute, National Institutes of Health, Bethesda, Maryland 20892-0520, USA.

Correspondence should be addressed to A.B. and G.M.C. *email: bax@nih.gov* and *clore@vger.niddk.nih.gov*

is included as a variable in the fit. As dipolar couplings are exquisitely sensitive to the orientation of the internuclear vector relative to the magnetic field, they potentially can improve considerably the accuracy of structures obtained by NMR methods.

Magnetic alignment

The anisotropy of a molecule's magnetic susceptibility tensor, $\underline{\chi}$, can be decomposed into the sum of an isotropic component, χ_o, and an anisotropic tensor, $\Delta\underline{\chi}$. The presence of anisotropy results in an orientation-dependent interaction energy, E, when the molecule is placed in a magnetic field:

$$E = -1/2\, B_o \cdot \Delta\underline{\chi} \cdot B_o / \mu_o \qquad (1)$$

where B_o is the strength of the magnetic field in tesla, and μ_o is the permeability ($\mu_o = 4\pi \times 10^{-7}$ tesla^2 m^3 joule^{-1}). For proteins in solution, E is much smaller than kT, and the magnetic susceptibility anisotropy results in only a very small degree of alignment with the magnetic field. As a consequence of this magnetic alignment, dipolar couplings no longer average to zero but have a small residual value which scales with the square of B_o. For small amplitude internal motions, the observed residual dipolar coupling (δ_{dip}) between nuclei A and B is given by[5]:

$$\delta_{dip}(\theta,\phi) = -C(B_o)\,[\chi_a(3\cos^2\theta - 1) + 3/2\,\chi_r(\sin^2\theta\cos 2\phi)] \qquad (2)$$

where $C(B_o)$ is $S(B_o^2/15kT)[\gamma_A\,\gamma_B\,h/(4\pi^2 r_{AB}^3)]$. S is the generalized order parameter for internal motions[7,10,12], γ_A and γ_B are the magnetogyric ratios of A and B; χ_a and χ_r are the axial and rhombic components of the magnetic susceptibility tensor ($\chi_a = \chi_{zz} - (\chi_{xx} + \chi_{yy})/2$; $\chi_r = \chi_{xx} - \chi_{yy}$), r_{AB} is the A–B internuclear distance, and θ and ϕ are cylindrical coordinates describing the orientation of the A–B vector in the principal axis system of the magnetic susceptibility tensor.

In isotropic solution, these small magnetic-field dependent dipolar splittings have been observed in a range of small molecules with relatively large magnetic shielding susceptibility anisotropy, such as polycyclic aromatics and porphyrins[4,5]. Considerably larger dipolar couplings are observed in molecules attached to discoidal micelle systems where the susceptibility anisotropy is summed over all the components of the micelle[13,14].

Equation (2) indicates that the dipolar interaction, $\delta_{dip}(\theta,\phi)$, is largest for small values of r_{AB} and large γ_A and γ_B. If these nuclei are also J coupled, with a coupling constant J_{AB}, the observed splitting equals the sum of the constant J_{AB} contribution and the magnetic field dependent dipolar interaction, $\delta_{dip}(\theta,\phi)$. In addition, there can be a very small magnetic field-dependent contribution resulting from relaxation interference effects[15], known as the dynamic frequency shift contribution, δ_{DFS}. The value of δ_{DFS} can be calculated accurately and, to a first approximation, is uniform for a given type of atom pairs, A and B (ref 7.).

Application to GATA–DNA complex

The magnetic susceptibility of most diamagnetic proteins is dominated by the aromatic groups of Phe, Tyr, Trp and His residues, and also contains contributions from the susceptibility anisotropies of the peptide bonds. Since the magnetic susceptibility anisotropy tensors of these individual contributors are generally not collinear, the net value of $\Delta\chi$ in diamagnetic proteins is usually small. Much larger values for $\Delta\chi$, however, are obtained if many aromatic groups are stacked in such a way that their magnetic susceptibility contributions are additive, such as found in nucleic acids[16]. For a protein–DNA complex, $\Delta\chi$ is therefore dominated by the DNA and to a good approximation will be axially symmetric, that is $|\chi_a| \gg |\chi_r|$. Under these conditions, the observed difference (ΔJ_{obs}) in J values at two field strengths will be given by:

$$\Delta J_{obs} = \Delta\delta_{DFS} - \Delta C(B_o)\,\chi_a\,(3\cos^2\theta - 1) \qquad (3)$$

To demonstrate the utility of Equation (3) in NMR structure determination and refinement, we have measured the magnetic-field dependent dipolar contributions to $^1J_{NH}$ and $^1J_{C\alpha H}$ splittings for a complex between the DNA-binding domain of the GATA-1 transcription factor and its cognate 16 base pair DNA fragment, for which a solution structure has been reported previously[17]. $^1J_{NH}$ splittings were measured at magnetic field strengths of 8.5, 14 and 17.5 T and exhibited the expected monotonic change with magnetic field strength. At 8.5 T, the two-dimensional ^{13}C–^1H correlation spectrum shows extensive overlap and measurements were therefore carried out at 11 and 17.5 T. Owing to the 2.5-fold larger

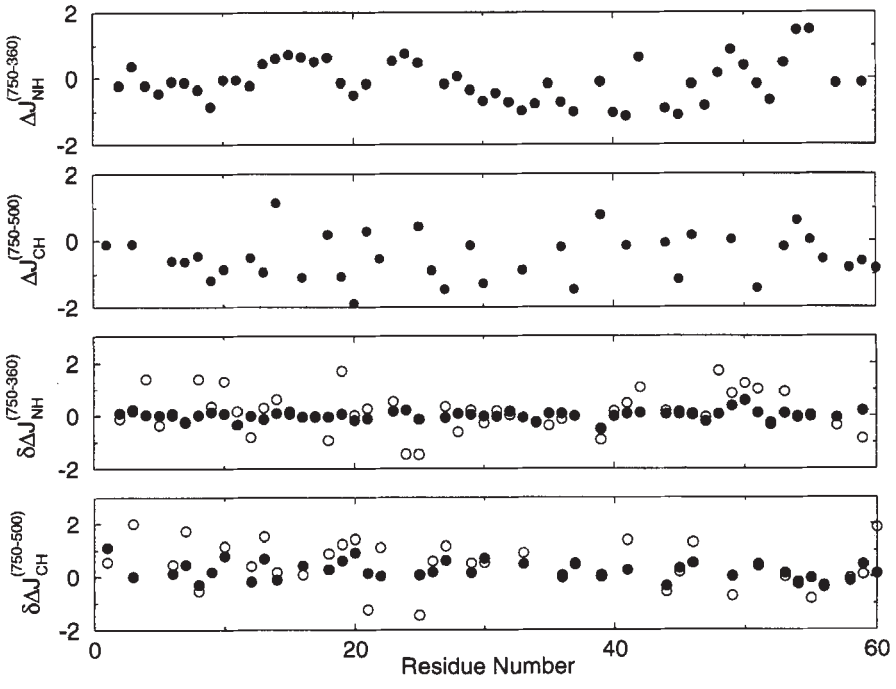

Fig. 1 Observed values of ΔJ_{NH}(750–360) and ΔJ_{CH}(750–500) (top two panels), and difference [$\delta\Delta J_{NH}$(750–360) and $\delta\Delta J_{CH}$(750–500)] between observed and calculated values of ΔJ_{NH}(750–360) and ΔJ_{CH}(750–500) (bottom two panels) obtained with (filled-in circles) and without (open circles) dipolar coupling restraints. Note that the 2D ^1H–^{13}C correlation spectrum shows extensive overlap at 360 MHz, so that $\Delta J_{C\alpha H}$ couplings were obtained from data recorded at 500 and 750 MHz.

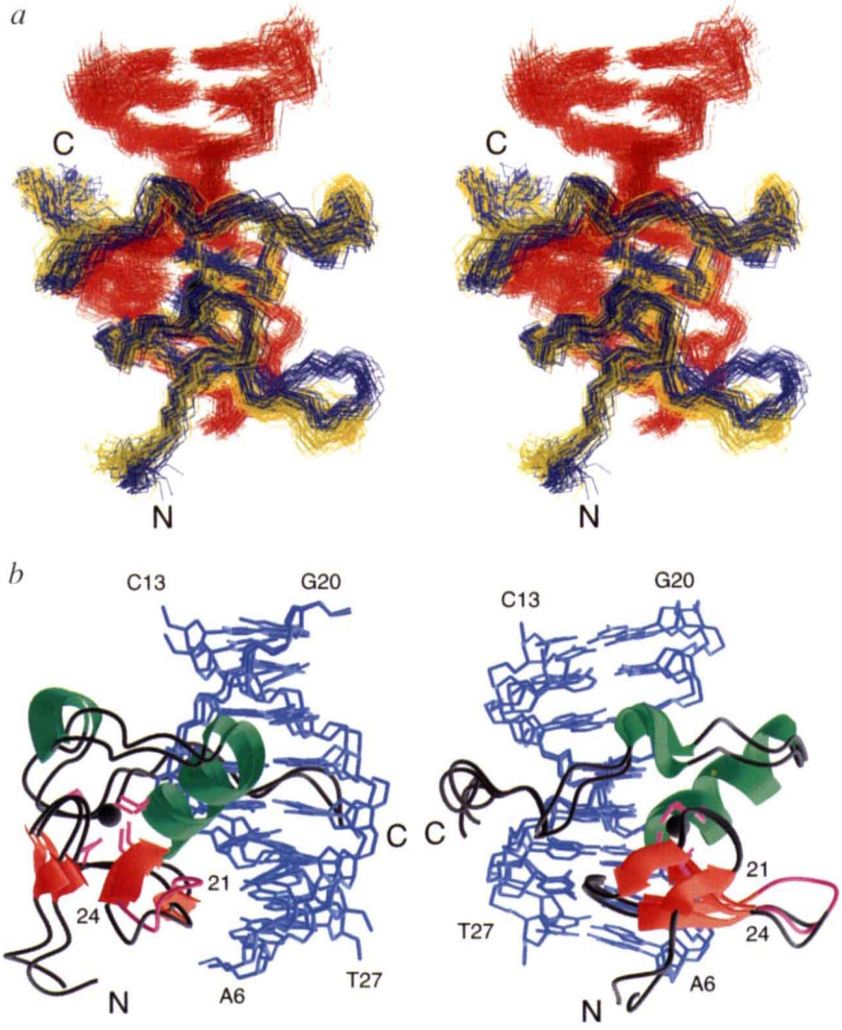

Fig. 2 ***a***, Stereoview showing a best fit superposition of the two ensembles of 30 simulated annealing structures obtained with (blue) and without (yellow) dipolar coupling restraints (the DNA for both ensembles is shown in red). ***b***, Two views showing best fit superpositions of the restrained regularized mean coordinates obtained with and without dipolar coupling restraints. The protein is shown as a ribbon diagram drawn through the Cα positions. The loop between strands β3 and β4 (residues 21–24) is shown in magenta for the structure obtained with dipolar coupling restraints, and in black for the structure obtained without dipolar coupling restraints.

magnetogyric ratio of ^{13}C relative to ^{15}N, which is partially offset by the 1.07-fold greater internuclear distance and the smaller range of magnetic fields, pairwise differences between $^1J_{CH}$ values measured at the two fields are nearly two-fold larger than for $^1J_{NH}$. However, the faster transverse relaxation of ^{13}C results in lower accuracy of the $^1J_{CH}$ splittings and higher uncertainties in the ^1H–^{13}C dipolar couplings (± ~0.2 Hz) compared to ^1H–^{15}N (± ~0.1 Hz).

No dipolar coupling restraints were obtained for residues with overlapping ^{15}N–^1H or $^{13}C\alpha$–^1H resonances, and dipolar coupling restraints for residues which experience either slow conformational exchange (resulting in vanishingly weak ^{15}N–^1H correlations) or low order parameters ($S^2 \leq 0.6$, that is $S \leq 0.77$) were also omitted. As a result, 52 out of a possible 62 ΔJ_{NH} and 38 out of a possible 66 $\Delta J_{C\alpha H}$ dipolar coupling restraints were available for analysis.

^{15}N T_1 and $T_{1\rho}$ experiments indicated that, with the exception of Lys 1, Gly 50 and the C terminus from Lys 61–Arg 66, all protein residues have S^2 values larger than 0.6, that is $S > 0.77$. Rather than using residue-specific S values, which include experimental uncertainty, only residues for which $S^2 > 0.6$ were considered and for these, all S values were assumed to be the same. Considering that $\delta_{dip,obs} = \delta_{dip,static}S$ and that peptide backbone amide S^2 values in structured regions of a protein typically fall in the 0.85 ± 0.05 range, the assumption of a uniform S value introduces a negligible error of at most a few percent in the dipolar coupling. Structure calculations with residue-specific S values yield results indistinguishable, from those obtained with uniform S values. In order to demonstrate that analysis of protein backbone mobility is not a prerequisite for the use of dipolar couplings, the results reported in this study are based on the use of a uniform S value. For values of the angle θ close to either 0° or 90°, the assumption of uniform values of S could in principle introduce errors in θ of greater than 5°. In practice, however, it has no effect on the calculated structures. This is due to the fact that the force, which is proportional to the gradient $\partial\Delta J/\partial\theta$, exerted during simulated annealing on the N–H or C–H vectors at $\theta = 0 \pm 10°$ or $90 \pm 10°$ is negligible and has a value of zero at $\theta = 0°$ and 90°.

Fig. 1 shows the variation as a function of residue number in the observed values of $\Delta J_{NH}(750–360)$ and $\Delta J_{C\alpha H}(750–500)$ for the backbone amide and CαH groups respectively. The contribution of $\Delta\delta_{DFS}$ to $\Delta J_{NH}(750–360)$ is calculated to be –0.06 Hz, using a rotational correlation time of 10.5 ns determined from ^{15}N relaxation measurements. As a result of the small $^{13}C\alpha$ chemical shift anisotropy, the value of $\Delta\delta_{DFS}$ is negligible for the case of $\Delta J_{C\alpha H}(750–500)$ and can therefore be ignored. The magnetic susceptibility tensor for the complex is dominated by contributions of the bases in the DNA duplex, yielding an axially symmetric susceptibility tensor with $\chi_a < 0$ and its unique axis approximately parallel to the axis of the double helix. The $\Delta J_{NH}(750–360)$ values for the residues in the recognition α-helix (residues 28–38) all are of similar magnitude, as expected for an α-helix for which the N–H vectors are aligned roughly parallel to the α-helix axis. They are all small and negative which indicates that, as expected, the recognition α-helix is oriented at an angle of ~60° relative to the long axis of the DNA.

Structure calculation with dipolar coupling

The geometric content of the dipolar couplings can be incorporated into the simulated annealing protocol[18] used for structure determination by minimizing the term $E_{dipolar}$:

$$E_{dipolar} = k_{dipolar}(\Delta J_{calc} - \Delta J_{obs})^2 \quad (4)$$

(where $k_{dipolar}$ is a force constant and ΔJ_{obs} and ΔJ_{calc} are the observed and calculated values of ΔJ respectively), in addition to

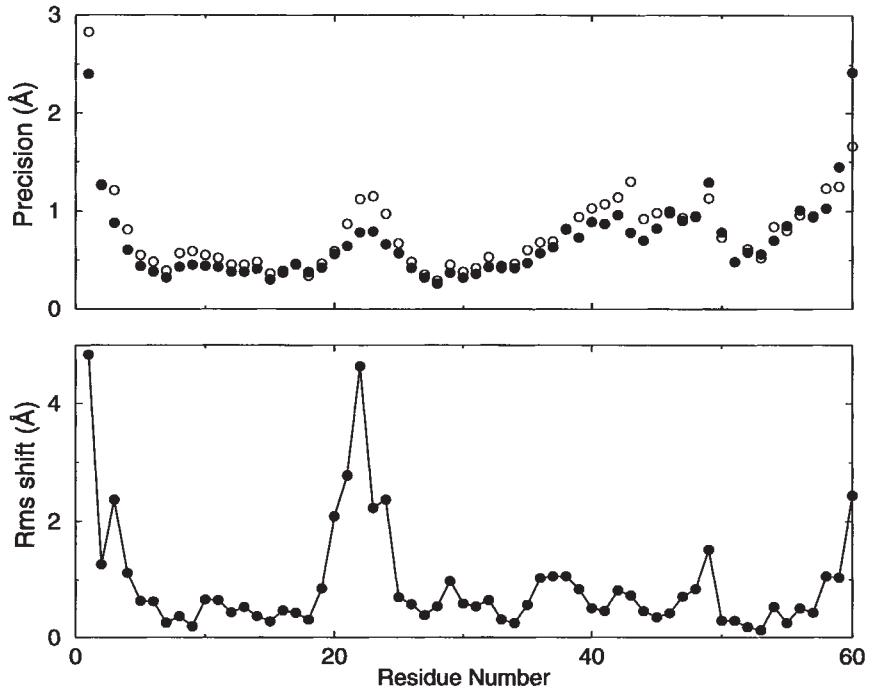

Fig. 3 Precision of the backbone (N, Cα, C, O) coordinates (top panel) and atomic r.m.s. shift for the backbone coordinates (bottom panel) between the average structures obtained with and without dipolar coupling restraints. The precision of the coordinates is given by the average r.m.s. shift between the 30 simulated annealing structures and their mean coordinate positions. The precision of the coordinates obtained with and without dipolar coupling constraints are shown as closed and open circles respectively. For any given residue, the difference between the two sets of structures is only significant when the atomic r.m.s. shift between the two mean coordinates for that residue exceeds the value for the corresponding sum of the coordinate precision for the two ensembles. Thus, the only region of significant difference lies in the loop (residues 21–24) connecting strands β3 and β4.

the various other terms in the target function for the distance and torsion angle restraints, covalent geometry and non-bonded contacts. $E_{dipolar}$ is evaluated by calculating the angles between the N–H and Cα–H bond vectors and an external arbitrary axis, defined by a single C–C bond positioned 50 Å away from the complex[3]. The value of the force constant $k_{dipolar}$ is chosen such that the agreement between observed and calculated ΔJ values is approximately equal to the experimental error. In this particular case, the target errors for ΔJ_{NH} and $\Delta J_{C\alpha H}$ are ~0.1 and ~0.2 Hz respectively. Empirically we found that these target errors were best achieved using force constants of 50 kcal mol^{-1} Hz^{-2} and 12.5 kcal mol^{-1} Hz^{-2} for ΔJ_{NH} and $\Delta J_{C\alpha H}$ respectively.

To apply Equation (4), the value of χ_a in Equation (3) must be determined directly from the ensemble of measured ΔJ values. χ_a has a maximum value of $-2\Delta C(B_o)\chi_a$ when the vector is parallel to the unique axis of the magnetic susceptibility tensor, and a minimum value of $+\Delta C(B_o)\chi_a$ when the vector is orthogonal to it (note that $^1J_{NH} < 0$ and $\chi_a < 0$). The probability of finding an N–H bond vector making an angle θ with the unique axis of the susceptibility tensor is proportional to sinθ, and very few N–H vectors are therefore expected to point parallel to this axis[3]. In contrast, a substantial fraction will be oriented nearly orthogonal to it[3], exhibiting a dipolar contribution of $\sim\Delta C(B_o)\chi_a$ to the $^1J_{NH}$ splitting. The value of $\Delta\delta_{DFS}$ can be accurately predicted from the measured ^{15}N relaxation times[7], and the magnitude of χ_a is then estimated by assuming that the five residues exhibiting the largest decrease in $^1J_{NH}$ with increasing field correspond to N–H vectors orthogonal to the unique axis of the magnetic susceptibility tensor. This yields a χ_a value of -24.4×10^{-34} m^3 $molecule^{-1}$ for the GATA-1/DNA complex, assuming a uniform S value of 0.92 (see above). Test calculations indicate that changes in χ_a by up to ±15% have a negligible effect on the calculated structures. We also note that in the case of a fully asymmetric magnetic susceptibility tensor, the rhombic component χ_r is readily obtained by carrying out a series of trial calculations for a small number of different rhombicities, in a manner exactly analogous to that previously described for obtaining the rhombic component of the diffusion tensor in heteronuclear relaxation refinement[3].

A summary of the statistics of the structures calculated with and without the dipolar coupling restraints is provided in Table 1, and a plot of the agreement between observed and calculated ΔJ values is shown in Fig. 1. A stereoview showing the best fit superpositions of an ensemble of 30 simulated annealing structures calculated with and without the dipolar coupling restraints is shown in Fig. 2*a*, and two views showing best-fit superpositions of the average structures are shown in Fig. 2*b*. The precision of the backbone atomic coordinates of the two ensembles of structures, and the atomic r.m.s. shift between the two mean coordinate positions is plotted as a function of residue in Fig. 3.

Effect of dipolar coupling on calculated structure

When the angle between the internuclear vector and the unique axis of the susceptibility tensor falls in the 20–70° range (or in the 110–160° range), the dipolar coupling is a very steep function of this angle. It is therefore not surprising that, prior to incorporation of the dipolar coupling restraints, agreement between the observed and predicted dipolar couplings is relatively poor (Table 1). When the dipolar coupling restraints are incorporated into the target function, agreement within experimental error is obtained between the observed and calculated values of both ΔJ_{NH} and $\Delta J_{C\alpha H}$ (Table 1). For the most part, this results in only small local structural changes. Thus, the orientation of GATA-1 on the DNA is the same in the two ensembles of structures. Moreover, the agreement with the other experimental data (NOE-derived approximate interproton distance restraints and torsion angle restraints) and the covalent geometry is only marginally affected by the incorporation of the dipolar coupling restraints (Table 1). The overall precision of the coordinates increases only slightly by the introduction of the dipolar coupling restraints (Table 2), but the quality of the backbone is improved significantly (Table 1).

In the mean refined structure, the angle between the DNA helix axis and the C–C vector employed as the magnetic susceptibility axis in the simulated annealing calculations is ~10°, confirming that the magnetic susceptibility tensor of the protein–DNA complex is indeed dominated by the DNA and is approximately collinear with the DNA axis.

Table 1 Summary of structural statistics[1]

	Without Dipolar Couplings <SA>	With Dipolar Couplings <$SA_{dipolar}$>
R.m.s. deviations from expt distance restraints[2] (Å) (1470)	0.044±0.001	0.047±0.001
R.m.s. deviations from expt dihedral restraints[2] (°) (296)[2]	0.233±0.041	0.359±0.061
Deviations from dipolar couplings		
^1H–^{15}N (Hz) (52)	0.510±0.032	0.084±0.005
^1H–^{13}C (Hz) (38)	0.653±0.055	0.214±0.017
Deviations from covalent geometry		
bonds (Å) (3257)	0.005±0.0000	0.005±0.0000
angles (°) (5895)	1.037±0.006	1.079±0.007
impropers (°) (1640)	0.328±0.036	0.430±0.036
Structure quality[3]		
% residues in most favourable region of Ramachandran map	62.0±4.6	78.7±2.8
Number of bad contacts per 100 residues	17.0±3.1	9.8±3.0

[1]<SA> and <$SA_{dipolar}$> are the ensembles of 30 simulated annealing structures calculated without and with the dipolar coupling restraints respectively. The number of terms for the various restraints is given in parentheses.
[2]None of the structures exhibited distance violations greater than 0.5 Å or dihedral angle violations greater than 5°. The experimental distance and torsion angle restraints were taken from reference 15 and have the accession code 1GAT_MR. The experimental distance restraints comprise 117 intermolecular interproton distance restraints between the protein and DNA, 919 intramolecular interproton distance restraints within the protein [comprising 334 intraresidue restraints, and 242 sequential, 161 short range ($1 < |i - j| \leq 5$) and 182 long range ($|i - j| > 5$) interresidue restraints], 26 loose restraints for 13 intraprotein hydrogen bonds, 371 intramolecular interproton distance restraints within the DNA [comprising 157 intraresidue, 180 sequential intrastrand, and 34 interstrand restraints], and 37 distance restraints for Watson-Crick hydrogen bonds within the DNA. The 144 torsion angle restraints for the protein consist of 58 ϕ, 56 ψ, 26 χ_1 and 4 χ_2 angles; the 152 torsion angle restraints for the DNA comprise loose restraints on the backbone α, β, γ, ε, and ζ angles to prevent problems associated with local mirror images.
[3]Calculated using the program PROCHECK[22].

With the exception of a single region, the ensembles of structures calculated with and without dipolar couplings overlap (Figs 2*a* and 3). There is, however, a large displacement (accompanied by a maximal ~4 Å r.m.s. shift in the backbone coordinates of residue 22) in the short loop (residues 21–24) which connects strands β3 and β4. Since this loop has low mobility, as judged from ^{15}N relaxation data, this observation illustrates one of the principal shortcomings of NMR structure determination based on NOE measurements. The only NOEs observed for residues 22 and 23 are either intraresidue or sequential, and there are no long range NOEs involving residues 21–24. Hence, the precision of the backbone coordinates for this loop is lower than that for the α-helix and β-strands (Fig. 3). Even though there are loose torsion angle restraints for the φ and ψ angles of these residues, accumulation of errors in the experimental restraints (for example, an NOE interproton distance restraint that is slightly too short, even by as little as 0.1 Å) becomes an important factor in determining the orientation of this loop with respect to the rest of the protein. The importance of the dipolar couplings is that by measuring the angle between the N–H and Cα–H bond vectors and the magnetic susceptibility tensor, they provide information on long range order, and hence can correctly orient such a loop, even in the absence of long-range interproton distance contacts. Indeed, in the ensemble of structures calculated without dipolar coupling restraints, amongst the largest deviations between observed and calculated values of ΔJ_{NH} and $\Delta J_{C\alpha H}$ are observed in the region comprising residues 19–25.

Several of the dipolar couplings measured for residues 19–25 are larger than predicted by the original structure, or have opposite signs. This then excludes the possibility that the change in orientation of this loop region is a result of motional averaging on a microsecond time scale, invisible to NMR relaxation experiments[10]. Such motions would reduce the magnitude of the observed dipolar couplings; a significant shift in the average orientation is needed to change the sign of the dipolar coupling, or to result in a dipolar coupling larger than predicted by the original structure.

It is worth noting that the structural changes in the loop comprising residues 21–24 observed upon dipolar coupling refinement are not dependent on having both ΔJ_{NH} and $\Delta J_{C\alpha H}$ restraints. An ensemble of structures was also calculated using only ΔJ_{NH} dipolar coupling restraints. The precision of the structures is unaffected, the atomic r.m.s. difference between the mean coordinates calculated with only ΔJ_{NH} and both ΔJ_{NH} and $\Delta J_{C\alpha H}$ restraints is only 0.53 Å for the protein backbone (residues 2–59), which is well within the overall precision of the coordinates (~0.7 Å), and the backbone atomic positions of residues 19–25 are identical in the two ensembles of structures. Thus, long range order can be defined using ΔJ_{NH} dipolar coupling restraints alone. The quality of the backbone is also improved upon refinement against only ΔJ_{NH} dipolar couplings, but not quite to the same extent as upon refinement against both ΔJ_{NH} and $\Delta J_{C\alpha H}$. Specifically, the number of bad contacts per 100 residues for the two ensembles of structures obtained upon refinement against only ΔJ_{NH} and both ΔJ_{NH} and $\Delta J_{C\alpha H}$ restraints is comparable (~11 *versus* ~10), and about two-fold lower than for the structures obtained without dipolar coupling refinement (~17). The percentage of residues, however, lying in the most favourable region of the Ramachandran plot in the ensemble of structures calculated with only ΔJ_{NH} restraints (~71%) is intermediate between that for the ensemble of structures calculated without dipolar coupling restraints (~62%) and with both ΔJ_{NH} and $\Delta J_{C\alpha H}$ restraints (~79%). This is hardly surprising, since the orientations of the N–H and Cα–H vectors in a dipeptide segment provide more restrictive restraints on φ and ψ than those of the N–H vectors alone.

Concluding remarks

We have demonstrated that small residual dipolar couplings in one-bond coupling constants can be measured in solution and used as structurally important restraints in NMR structure determination. The method is most suitable for systems with relatively large values of the magnetic susceptibility tensor. This includes protein–nucleic acid complexes, nucleic acids, proteins with large numbers of aromatic residues, porphyrin containing proteins, metal binding proteins where the natural metal, if diamagnetic, can be replaced by a lanthanide, and proteins chemically modified to artificially increase the magnitude of the magnetic susceptibility tensor (for example, by binding lanthanides).

In the case of protein–DNA complexes, the introduction of dipolar coupling restraints aids the determination of the orientation of the protein relative to the long axis of the DNA. Likewise, for multidomain proteins, multimeric proteins and

Table 2 Precision of atomic coordinates and atomic r.m.s. shifts[1]

	Coordinate precision (Å)		Atomic r.m.s. shift (Å)
	<SA> *versus* $\overline{SA}$	<$SA_{dipolar}$> *versus* $\overline{SA}_{dipolar}$	$\overline{SA}$ *versus* $\overline{SA}_{dipolar}$
Protein backbone + Zn + DNA	0.69±0.12	0.67±0.09	0.78
All protein atoms + DNA	1.07±0.10	1.01±0.11	0.99
Protein backbone	0.76±0.13	0.68±0.15	1.12
All protein atoms	1.29±0.13	1.21±0.15	1.25
DNA	0.62±0.16	0.65±0.10	0.39

[1]<SA> and <$SA_{dipolar}$> are the ensembles of 30 simulated annealing structures calculated without and with dipolar coupling restraints respectively. $\overline{SA}$ and $\overline{SA}_{dipolar}$ are the respective average coordinates calculated from each ensemble (obtained by best fitting residues 2–59 of the protein, the Zn atom, and base pairs 6–13 of the DNA). The atomic r.m.s. values given are for residues 2–59 of the protein, the zinc atom and base-pairs 6–13 of the DNA. Residues 1 and 60–66 of the protein are disordered, and basepairs 1–5 and 14–16 are not in contact with the protein so that their conformation is only restrained by sequential NOEs.

protein–protein complexes, dipolar couplings should provide a powerful tool for determining relative orientations and mobilities of the various components. Recently, it has been demonstrated that very low resolution structures can be obtained from NMR data for slowly tumbling proteins with relative molecular masses larger than 30,000 if uniform ^2H enrichment is used, in the presence of selected protonated groups (specifically amides and methyl groups) for which a small number of NOE-derived interproton distances can be obtained[19,20]. It is likely that a combination of this approach together with the measurement of dipolar couplings for the backbone atoms will result in considerably better definition of such larger proteins. For larger proteins limited spectral resolution could potentially hinder the measurement of an increasingly large number of dipolar couplings. This problem, however, can be alleviated or circumvented using one of several different approaches. These include perdeuteration of non-exchangeable protons to narrow the linewidths, thereby increasing the resolution; the use of amino acid-specific labeling to simplify the spectrum; and the use of three-dimensional NMR to increase the spectral resolution by separating the ^1H–^{15}N or ^1H–$^{13}C\alpha$ correlations according to the chemical shift of a third nucleus (for example, the carbonyl carbon).

The degrees of magnetic alignment utilized in the present study are extremely small, and Brownian motion reduces the dipolar couplings for the protein–DNA complex used in this study by a factor of ~10^4 relative to the static values. The degree of magnetic alignment increases with the square of the field strength, and the development of even stronger magnetic fields will therefore widen the applicability of dipolar coupling measurements to systems with smaller magnetic susceptibility anisotropy. In addition, it is possible to exploit a protein's anisotropic electrical polarizability tensor or optical absorption tensor to obtain considerable degrees of alignment of proteins by means of strong low frequency electric fields or by the use of polarized light.

Methods

All NMR experiments were carried out at pH 6.5 on a 2 mM complex containing a molar ratio of 1:1.1:1 of chicken GATA-1 DNA binding domain uniformly (>95%) labelled with ^{15}N or $^{15}N/^{13}C$, zinc, and double-stranded 16-bp oligonucleotide at natural abundance. Samples were purified and prepared as described[17]. NMR resonance assignments were taken from ref. 17.

Measurement of $^1J_{NH}$ couplings was carried out at 25 °C on three different Bruker NMR spectrometers, an AMX360, a DMX600 and a DMX750, operating at ^1H frequencies of 360, 600 and 750 MHz respectively. The $^1J_{NH}$ values were extracted from *J*-modulated signals as described[7], using effective modulation delays of 34.7, 35.5, 36.9, 38.3, 39.7, 45.9, 46.8, 47.7, 49.3, and 50.4 ms. The total acquisition time for each modulation delay was two hours. The measurements at 360 and 750 MHz were carried out twice at each field and yielded a pairwise r.m.s. reproducibility in $^1J_{NH}$ of 0.18 and 0.12 Hz for the 360 and 750 MHz data respectively. This corresponds to random uncertainties of 0.09 (360 MHz) and 0.06 Hz (750 MHz) in the averaged values[7] which were used in subsequent calculations.

The $^1J_{CH}$ couplings were measured in a similar fashion, using a slightly modified constant-time version of the ^1H–^{13}C HSQC experiment[8]. The experiments were carried out at 40 °C on two Bruker NMR spectrometers, a DMX500 and a DMX750 with ^1H frequencies of 500 and 750 MHz respectively. The $^1J_{CH}$ modulation delays used were 23.48, 23.80, 24.13, 24.47, 24.82, 25.17, 25.54, 25.92, 26.31, and 27.96 ms. The total acquisition time for each modulation delay was two hours. Duplicate measurements were performed and indicate pairwise r.m.s. differences for $^1J_{CH}$ of 0.36 and 0.28 Hz for the 500 and 750 MHz data respectively, and random errors of 0.18 and 0.14 Hz in the averaged values. The average values of $^1J_{NH}$ and $^1J_{CH}$ from the duplicated experiments were used in the subsequent calculations.

Structures were calculated by simulated annealing[18] using the program X-PLOR[21] modified to incorporate dipolar coupling restraints. The target function that was minimized comprised quadratic square-well potentials for the interproton distance and torsion angle restraints, harmonic potentials for the dipolar coupling restraints and covalent geometry (bonds, angles and improper torsions which define planarity and chirality), and a quartic van der Waals repulsion term for the non-bonded contacts. No empirical hydrogen bonding, electrostatic or Lennard-Jones potential terms were included in the calculations. The final values of the force constants for the various terms are as follows: 30 kcal mol^{-1} $Å^{-2}$ for the interproton distance restraints; 200 kcal mol^{-1} rad^{-2} for the torsion angle restraints; 50 kcal mol^{-1} Hz^{-2} and 12.5 kcal mol^{-1} Hz^{-2} for the ΔJ_{NH} and ΔJ_{CH} dipolar coupling restraints; 1000 kcal mol^{-1} $Å^{-2}$ for bonds and 500 kcal mol^{-1} rad^{-2} for bond angles and improper torsions; and 4 kcal mol^{-1} $Å^{-4}$ with a van der Waals radius scale factor of 0.8 (employing the CHARMM PARAM19/20 van der Waals radii) for the van der Waals repulsion term. The values of $k_{dipolar}$ were chosen to reflect the uncertainty in the values of the measured dipolar couplings and the two-fold larger uncertainty in the ΔJ_{CH} versus the ΔJ_{NH} values. The starting coordinates for the simulated annealing calculations were taken from the restrained regularized mean coordinates of the GATA-1/DNA complex[17] (PDB accession code 1GAT).

Without using the dipolar coupling restraints, adding the susceptibility tensors of the nucleic acid bases, peptide bonds, and aromatic residues yields $\chi_a = -22.9 \times 10^{-34}$ and $\chi_r = 1.9 \times 10^{-34}$ m^3 $molecule^{-1}$, with the unique axis of the axial component making an angle θ of 7° with the DNA axis; for the averaged structure calculated with the dipolar constraints included: $\chi_a = -23.0 \times 10^{-34}$ and $\chi_r = 1.0 \times 10^{-34}$ m^3/molecule, $\theta = 6°$. For comparison, the value of χ_a derived from the ensemble of ΔJ_{NH} values and used in the structure calculations is -24.4×10^{-34} m^3 $molecule^{-1}$.

Acknowledgements

We thank D. Garrett and F. Delaglio for software support, A. Szabo and J. Huth for useful discussions, and R. Tschudin for technical support. This work was supported by the AIDS-directed Antiviral Program of the Office of the Director of the National Institutes of Health (A.B., G.M.C. and A.M.G.).

Received 16 April 1997; accepted 7 July 1997.

1. Wüthrich, K. *NMR of Proteins and Nucleic Acids* (Wiley, New York; 1986).
2. Clore, G.M. & Gronenborn, A.M. Determination of three-dimensional structures of proteins and nucleic acids in solution by nuclear magnetic resonance spectroscopy. *CRC Crit. Rev. Biochem. Mol. Biol.* **24**, 479–564 (1989).
3. Tjandra, N., Garrett, D.S., Gronenborn, A.M., Bax, A. & Clore, G.M. Defining long range order in NMR structure determination from the dependence of heteronuclear relaxation times on rotational diffusion anisotropy. *Nature Struct. Biol.* **4**, 443–449 (1997).
4. Gayathri, C., Bothner-By, A. A., van Zijl, P.C. M. & MacLean, C., Dipolar magnetic field effects in NMR spectra of liquids. *Chem. Phys. Lett.* **87**, 192–196 (1982).
5. Bothner-By, A. A. Magnetic field induced alignment of molecules. In *Encyclopedia of Nuclear Magnetic Resonance* (eds Grant, D. M. & Harris, R.K.) 2932–2938 (Wiley, Chichester; 1995).
6. Tolman, J. R. & Prestegard, J. H. A quantitative *J*-correlation experiment for the accurate measurement of one-bond amide ^{15}N-^{1}H couplings in proteins. *J. Magn. Reson. B* **112**, 245–252 (1996).
7. Tjandra, N., Grzesiek, S. & Bax, A. Magnetic field dependence of nitrogen-proton *J* splittings in ^{15}N-enriched human ubiquitin resulting from relaxation interference and residual dipolar coupling. *J. Am. Chem. Soc.* **118**, 6264–6272 (1996).
8. Tjandra, N. & Bax, A. Measurement of dipolar contributions to $^{1}J_{CH}$ splittings from magnetic field dependence of *J* modulation in two-dimensional NMR spectra. *J. Magn. Reson.* **124**, 512–515 (1997).
9. Tolman, J. R., Flanagan, J. M., Kennedy, M. A. & Prestegard, J. H. Nuclear magnetic dipole interactions in field-oriented proteins: Information for structure determination in solution. *Proc. Natl. Acad. Sci. U.S.A.* **92**, 9279–9283 (1995).
10. Tolman, J. R., Flanagan, J. M., Kennedy, M. A. & Prestegard, J. H. NMR evidence for slow collective motions in cyanometmyoglobin. *Nature Struct. Biol.* **4**, 292–297 (1997).
11. Tjandra, N. & Bax, A. Are proteins even floppier than we thought? *Nature Struct. Biol.* **4**, 254–256 (1997).
12. Lipari, G. & Szabo, A. Model-free approach to the interpretation of nuclear magnetic resonance relaxation in macromolecules I: theory and range of validity. *J. Am. Chem. Soc.* **104**, 4546–4559 (1982).
13. Sanders, C. R., Hare, B. J., Howard, K. P. & Prestegard, J. H. Magnetically-oriented phospholipid micelles as a tool for the study of membrane-associated molecules. *Prog. Nucl. Magn. Reson. Spectrosc.* **26**, 421–444 (1994).
14. Salvatore, B. A., Ghose, R. & Prestegard, J. H. NMR studies of a ^{13}C,^{15}N-labeled G_{M4}-lactam glycolipid at an oriented model-membrane interface *J. Am. Chem. Soc.* **118**, 4001–4008 (1996).
15. Werbelow, L. G. in *Encyclopedia of Nuclear Magnetic Resonance* (eds Grant, D. M. & Harris, R.K.) 4072 (Wiley, Chichester; 1995).
16. Kung, H. C., Wang, K. Y., Goljer, I. & Bolton, P. H. Magnetic alignment of duplex and quadruplex DNAs. *J. Magn. Reson. Ser. B*, **109**, 323–325 (1995).
17. Omichinski, J.G., Clore, G.M., Schaad, O., Felsenfeld, G., Trainor, C., Appella, E., Stahl, S.J., Gronenborn, A.M. NMR structure of a specific DNA complex of a Zn-containing DNA binding domain of GATA-1 *Science* **261**, 438–446 (1993).
18. Nilges, M., Gronenborn, A.M., Brünger, A.T. & Clore, G.M. Determination of three-dimensional structures of proteins by simulated annealing with interproton distance restraints: application to crambin, potato carboxypeptidase inhibitor and barley serine proteinase inhibitor 2. *Protein Engng.* **2**, 27–38 (1988).
19. Metzler,W. J., Wittekind, M., Goldfarb, V., Mueller, L. & Farmer, B. T. Incorporation of ^{1}H/^{13}C/^{15}N-{Ile, Leu, Val} into a perdeuterated protein: Potential in structure determination of large proteins by NMR. *J. Am. Chem. Soc.* **118**, 6800–6801 (1996).
20. Gardner, K. H., Rosen, M. K. & L. E. Kay, Global folds of highly deuterated, methyl-protonated proteins by multi-dimensional NMR. *Biochemistry* **36**, 1389–1401 (1997).
21. Brünger, A.T. *XPLOR Manual Version 3.1* (New Haven, Connecticut: Yale University; 1993).
22. Laskowski, R.A., MacArthur, M.W., Moss, D.S. & Thornton, J.M. PROCHECK: a program to check the stereochemical quality of protein structures. *J. Appl. Crystallogr.* **26**, 283–291 (1993).